

# Gene clusters reflecting macrodomain structure respond to nucleoid perturbations<sup>†</sup>

Vittore F. Scolari,<sup>a,b,c</sup> Bruno Bassetti,<sup>c,d</sup> Bianca Scavi,<sup>e</sup> and Marco Cosentino Lagomarsino<sup>\*a,b,c</sup>

## Abstract

Focusing on the DNA-bridging nucleoid proteins Fis and H-NS, and integrating several independent experimental and bioinformatic data sources, we investigate the links between chromosomal spatial organization and global transcriptional regulation. By means of a novel multi-scale spatial aggregation analysis, we uncover the existence of contiguous clusters of nucleoid-perturbation sensitive genes along the genome, whose expression is affected by a combination of topological DNA state and nucleoid-shaping protein occupancy. The clusters correlate well with the macrodomain structure of the genome. The most significant of them lay symmetrically at the edges of the *ter* macrodomain and involve all of the flagellar and chemotaxis machinery, in addition to key regulators of biofilm formation, suggesting that the regulation of the physical state of the chromosome by the nucleoid proteins plays an important role in coordinating the transcriptional response leading to the switch between a motile and a biofilm lifestyle.

arXiv:1011.1280v1 [q-bio.GN] 4 Nov 2010

□ <sup>†</sup> Electronic Supplementary Information (ESI) available: on website <http://www.lgm.upmc.fr/scolarietal/>.

□ <sup>a</sup> Genomic Physics Group, FRE 3214 CNRS "Microorganism Genomics"

□ <sup>b</sup> Université Pierre et Marie Curie, 15 rue de L'École de Médecine Paris, France

□ <sup>c</sup> Università degli Studi di Milano, Dip. Fisica. Via Celoria 16, 20133 Milano, Italy

□ <sup>d</sup> I.N.F.N. Milano, Via Celoria 16, 20133 Milano, Italy

□ <sup>e</sup> LBPA, UMR 8113, ENS Cachan, 61, avenue du Président Wilson, 94235 Cachan, France

□ \* [ e-mail address:]Marco.Cosentino-Lagomarsino@upmc.fr

## Introduction

The success of a cell's survival under different growth conditions depends on its ability to regulate a coordinated transcriptional response to specific environmental changes or stresses, involving large groups of genes [1, 2]. In bacteria, transcriptional regulation of genes depends on the binding of proteins to DNA, but also on the physical configurations of the resulting mesoscopic protein/DNA complex, the nucleoid [3–5].

Specific nucleoid-shaping transcription factors (NSTFs) have the task of modulating the nucleoid's dynamic structure in response to changes in environmental conditions [6]. This can result, for example, in a change in the compaction of the chromosome and in a differential distribution of mechanical energy, stored as supercoiling. These changes in the physical properties of the DNA can affect the level of expression of specific genes, in parallel to the activity of specific transcription factors. NSTFs may thus change the expression of many genes (some of which may code for the same NSTFs) both directly and through the physical conformations that they induce on the genome [3].

The current transcription network view of gene regulation represents specific transcription-factor binding sites upstream of promoters as a directed graph, linking each transcription factor to its target node (which represents the transcript and its protein product) if the transcription factor has at least one binding site with documented activity in the cis-regulatory region of the target [7]. With this definition, the interaction graph structure is given by both large-scale experiments and collections of small-scale experiments [8]. This view considers the graph of all genome (transcriptional) interactions but completely disregards the effects on gene expression due to changes of the nucleoid. The role played by the nucleoid's structure in the hierarchy of events leading to large scale transcription patterns remains largely to be elucidated. In the near future it will be necessary to incorporate these into a generalized description of the organization of the genome and the regulatory network it encodes for. This is a challenging problem because the output of the transcription network is due to the sum of both local and global regulatory signals, from the biochemical properties of transcription factors, such as their concentration and affinity for the sites on the promoter, to the mesoscopic nucleoid organization and DNA conformational and topological states.

Nucleoid organization itself remains to be fully characterized. Most of NSTFs have been identified [6], and in some cases their local action is well known: for example, DNA bridging by H-NS or Fis is believed to be important for DNA loop stabilization [9]. Such supercoiled plectonemic loops can be topologically isolated from the rest of the genome, modulating protein binding and transcription rates [4]. On larger scales, meticulous recombination experiments have shown that the nucleoid as a polymer-protein complex is divided into six compartments, or “macrodomains” [10]. Four of these macrodomains are defined by pref-

erential interaction of DNA fragments within the same domain and by their spatial colocalization within the cell [10–12]. DNA segments within a macrodomain typically intersect, while inter-macrodomain collisions appear to be restricted. The two remaining “nonstructured regions” are more fluid in nature. Other experiments have probed large-scale nucleoid structure by tagging of specific loci and/or by nucleoid isolation [13–19]. GFP-RNAP fusions have also been used in this context in an effort to identify possible “transcription factories” [5, 20–22].

The relation between nucleoid state and gene expression has been the subject of several recent studies. Experimentally, this question has been addressed using mainly transcriptomics and chromatin immunoprecipitation combined with microarrays (ChIP-chip). Thanks to elegant experiments linking the length distribution of observed supercoiled domains with the transcriptional response to locally induced supercoil relaxation [23], we know that gene expression can be affected by its localization within such an isolated topological domain [24, 25]. Thus, the same bridging nucleoid proteins that give the nucleoid a branched structure when observed by electron microscopy may also be responsible for part of the transcriptional regulation not accounted for by the network of transcription factors and regulated genes. Other experiments have characterized RNA-polymerase (RNAP) and specific NSTF binding by ChIP-chip [26–28]. By monitoring generic protein binding throughout the chromosome [29], Vora *et Al.* have found extended protein binding regions (called “extended protein occupancy domains” or EPODs) connected to either transcriptionally silent or highly expressed clusters of genes. Finally, transcriptomics has been applied to the study of the effects of the knockout of specific bridging nucleoid protein and to changes in the level of negative supercoiling [30–32].

Computationally, attempts have been made to characterize the binding specificity of NSTFs [33, 34] and to interrogate the one-dimensional arrangement of genes of different categories for signals possibly related to nucleoid structure [35, 36]. In particular, a thread of studies [37–40] on possible “periodicity” patterns has found a number of interesting spatial regularities in the arrangement of genes belonging to different categories. For example, the correlation of gene expression with gene codon bias, has recently been related to large contiguous “sectors” along the chromosome [37].

Here, we present an integrated analysis combining different independent data sources that report on (i) specific DNA-protein interactions, (ii) different levels of gene expression, and (iii) large scale nucleoid structure, in order to uncover coherent, consistent correlations between these different levels of genome organization. We focus on the spatial distribution along the genome of these data sets. Our statistical aggregation analysis shows that part of the macrodomain structure of the genome emerges directly from the analysis of the distribution of genes that change their expression when comparing wild-type versus nucleoid-perturbed conditions [31]. In addition, by the analysis of specific nucleoid protein occupancy profiles and

EPODS, we recover a similar structure, where the most significant regions flank the Ter macrodomain of the nucleoid defined by Valens and coworkers [10]. In the same data, we also recover a periodicity signal in analogy with previous studies on other genomic data sources related to transcription of *E. coli* genes and genome adaptation. Finally, a functional analysis of the clusters reveals significant enrichment of the flagellar and chemotaxis genes, together with regulators of biofilm formation.

## I. RESULTS

### A. The distribution of genes sensitive to H-NS/Fis deletion and supercoiling perturbations is nonuniform along the genome.

We began the analysis from the transcriptomics data of Blot *et al.* [30, 31]. In these experiments the global expression profiles of wild-type *E. coli* K12 were compared with mutants carrying combined nucleoid perturbations in the form of knockouts of the NSTFs proteins Fis or H-NS, and a mutation of a gyrase or a topoisomerase, affecting the average supercoiling background. The differential analysis of these experiments gives seven sets of genes significantly responding to these nucleoid-related perturbations (Supplementary Figure SM1). A simple density map of these lists shows notable peaks that correspond to linear regions of the chromosome characterized by a stronger transcriptional reaction to nucleoid-related perturbations with respect to other parts of the chromosome.

### B. Clusters of transcriptional response to H-NS/Fis deletion and supercoiling perturbations correlate with macro-domain and chromosomal segment organization of the genome.

Marr and coworkers [31] detected clusters in the same gene lists with a threshold technique linking genes with the proximity threshold  $t$  in the range  $1b < t < 10Kb$ . We performed a different clustering analysis probing multiple scales, considering also the statistical significance of the one dimensional aggregation by comparing the peaks of the empirical histogram with the highest peak found in the histogram of randomized lists. Our method can thus define relevant clusters and also associate a  $P$ -value to them for every given scale (see Methods and Figure 1).

We systematically analyzed both supercoiling sensitive genes in the WT,  $\Delta$ Fis and  $\Delta$ H-NS intra-strain lists (see Methods) and the nucleoid-protein sensitive genes at fixed supercoiling condition in the WT- $\Delta$ Fis(low  $-\sigma$ ), WT- $\Delta$ Fis(high  $-\sigma$ ), WT- $\Delta$ H-NS(low  $-\sigma$ ), WT- $\Delta$ H-NS(high  $-\sigma$ ) inter-strain lists. Supplementary Figure S1 shows the clusters found. A cluster at 1.90-1.96 Mb, or 41 centisomes ( $P = 0.01$ )

of genes sensitive to supercoiling changes was found for all three strains. Another cluster at 1.10-1.20 Mb, 24 centisomes, ( $P < 10^{-3}$ ) sensitive to supercoiling changes appears in the wild type experiment, and a cluster at 3.80-3.81 Mb, 82 centisomes ( $P = 0.04$ ) is present in the mutant lacking the Fis protein. The deletion of Fis at fixed supercoiling background causes a variation in gene expression in a cluster at 1.95-2.03 Mb, 43 centisomes, ( $P = 0.05$ ) in both high and low negative supercoiling conditions and in a cluster at 3.33-3.55 Mb, 74 centisomes ( $P = 0.01$ ) only at low negative supercoiling conditions. The deletion of H-NS at fixed supercoiling background causes the emergence of a pair of neighboring clusters respectively at 1.97-2.05 and 2.08-2.15 Mb (around 43 centisomes) and a cluster at 1.06-1.17 Mb (24 centisomes) at both supercoiling conditions ( $P < 10^{-3}$ ). Another cluster emerges in the condition of low negative supercoiling at 1.50-1.66 Mb (34-35 centisomes,  $P = 0.03$ ), a position compatible with the replication terminus, and a cluster at 0.30-0.34 Mb, 7 centisomes, ( $P = 0.05$ ) appears at high negative supercoiling condition. Notably, very similar clusters appear from the data on the genes significantly responding to Fis deletion as a function of the growth phase, specifically in mid exponential phase [32] (Supplementary Figure S2).

A summary of the most significant clusters is shown in Figure 2 and Supplementary Table S1. At the scale of the macrodomains, these clusters appear to overlap well with the previously observed segmented structure of the chromosome [10, 37]. At smaller scales, clusters preferentially localize towards the edges of macrodomains or in nonstructured regions (Supplementary Figures S1 to S3). In particular, the highest significance clusters appear at all scales in H-NS-related perturbation experiments as well as in response to supercoiling changes in the intra-strain WT list (see Figure 2). At small scales, these clusters concentrate rather well, within the uncertainty of the analysis, to the edges of the Ter macrodomain defined by Boccard and coworkers [10, 13], also termed fluid region by a more recent study [14], while at larger scales they cover the entire Ter macrodomain.

### **C. Binding profiles of nucleoid-shaping proteins along the genome follow the same spatial patterns of the expression data.**

The previous analysis shows a tight link of the transcription program with the structuring of the nucleoid, and the macrodomains in particular, related to the action of the NSTFs Fis and H-NS. In order to test for the direct action of these proteins at these sites, we considered data concerning specific binding sites of Fis and H-NS on the chromosome. Binding sites of H-NS and Fis proteins along the *E. coli* genome *in vivo* were extracted from the ChIP-chip data of Grainger *et al.* [27]. We also considered the list of FIS binding sites obtained by high-density ChIP-chip by Cho *et al.* [28] and from the RegulonDB database [8] (see methods for the nomenclature of these experiments).

The cluster diagrams of those lists are reported in Supplementary Figure S3. The clearest clusters appear from the experiments of Grainger and coworkers. In particular, we found three clusters with a low  $P$ -value ( $P < 10^{-3}$ ) in FISbind(Grainger) of which two (at 1.12-1.14 Mb, 24 centisomes, and at 1.95-2.03 Mb, 43 centisomes) that are precisely superimposed on the clusters found in Wt- $\Delta$ H-NS gene expression data sets, laying at the border of the Ter macrodomain, and one (at 3.43-3.46 Mb, 74 centisomes) corresponding to the cluster already found in WT- $\Delta$ Fis. We also found two clusters in HNSbind(Grainger) at 1.99-2.02 Mb, 43 centisomes ( $P < 10^{-3}$ ) and at 2.09-2.12 Mb, 45 centisomes ( $P = 0.01$ ) that correspond to the cluster found in the transcriptomics in Wt- $\Delta$ H-NS set, at the border of the Ter macrodomain. Finally, we find a cluster at 2.98-3.00, 64.5 centisomes ( $P = 0.01$ ) and another one at 3.78-3.82, 82 centisomes ( $P < 10^{-3}$ ) that can be superimposed with the border of the Ori macrodomain. The Fis binding data of Cho *et al.* appear to give a weaker signal for this cluster, which however remains visible. This discrepancy may come from the different resolution of the two studies, or from a different threshold used in the two studies to define a binding site. Finally, the other control set from H-NS high-resolution binding data from Oshima *et al.* shows all the clusters found in the Grainger data, plus additional clusters, especially found in the Ter area. In this case, the differences are most likely due to the different growth conditions in this experiment.

Considering Fis and H-NS binding sites from the RegulonDB dataset, we found multiple clusters of difficult interpretation. This is possibly due to the knowledge bias of those data and the elusive nature of NSTF binding motifs [33]. Sonnenschein and coworkers [36] found that genes that, according to current knowledge as compiled by RegulonDB, do not participate in the transcriptional regulatory network, show a statistical repulsion for linear genome positioning with genes that do, and they interpret this as a signature of nucleoid-related gene regulation. Motivated by this finding, we also performed a comparative cluster analysis on the genes included in the RegulonDB regulatory network and outside (Supplementary Figure S4). While the knowledge-biased RegulonDB network presents many clusters of difficult interpretation, we surprisingly found that the genes outside the RegulonDB network show clear clusters on the border of the Ter macrodomain and a larger scale cluster covering the Ter macrodomain ( $P < 10^{-3}$ ). These regions might be enriched of genes expressed under physical control by the nucleoid rather than by specific network interactions. Alternatively, the unknown function of some of these operons results in a lack of information regarding their regulatory mechanisms.

In order to gain more insight into the binding of nucleoid related proteins on the DNA, we also considered the extended protein occupancy domains (EPOD) experimental data produced by Vora *et al* [29]. This technology reveals protein occupancy across an entire bacterial chromosome at the resolution of individual binding sites. EPODs are long contiguous segments of DNA-bound proteins along the chromosome, and were found to correspond to transcriptionally silent region (tsEPODs) or highly expressed ones (heEPODs).

We compared the density profiles of heEPOD and tsEPOD to the gene density of the other data sets. The local contributions to the Pearson correlation coefficient of some representative data sets are plotted in Supplementary Figure S6. The figure shows a high correlation between heEPOD density, FISbind(Grainger) and WT- $\Delta$ H-NS(low  $-\sigma$ ), specifically in the area around the border of the Ter macrodomain (around 2Mb, or 43 centisomes). The similarity of the density profile is evident from the visual inspection of the normalized densities. As an example, Figure S5 reports the case of heEPOD and WT- $\Delta$ H-NS(low  $-\sigma$ ). Finally, we considered the enrichment of lists of genes within EPODs with respect to genes responding to nucleoid perturbations (Supplementary table S2 and S3). heEPODs have a significant intersection with all the inter-strain experiments as well as with the intra-strain supercoiling changes in absence of H-NS. On the other hand, tsEPODs significantly overlap only with the perturbation experiments related to H-NS (inter-strain), as expected from its known role as a transcriptional repressor [41, 42].

#### **D. Functional classes of genes in the clusters.**

Hypergeometric testing of enrichment for MultiFun [43] functional categories was carried out systematically to all the considered datasets and also to the genes contained in the most significant clusters found in the spatial aggregation analysis. The result of the enrichment analysis are available on the web site <http://www.lgm.upmc.fr/scolarietal/>.

The flagella and chemotaxis classes, in addition to several biofilm related classes, are enriched in both of the clusters at the edges of the Ter macrodomain (Cluster 1 and Cluster 4). These classes are also enriched in the following datasets: FISbind (Grainger), HNSbind (Grainger)  $\Delta$ Fis intra-strain, WT- $\Delta$ Fis and WT- $\Delta$ H-NS at both supercoiling conditions, WT- $\Delta$ H-NS (ME), and WT- $\Delta$ Fis (150 and 240min) in the Bradley data sets. In order to compare these clusters the flagella synthesis network, we carried out a spatial aggregation analysis of the operons directly controlled by the FlhC transcription factor, the master regulator of flagella gene expression. The cluster diagram is reported in Supplementary Figure S7 and shows a clear correlation with the clusters identified by the analysis of the datasets from both Fis and H-NS binding and transcriptomics experiments.

The role of Fis and H-NS in the regulation of flagellar gene expression has been known for some time [44–47]. Interestingly, flagella and chemotaxis genes share the same clusters with functional classes related to biofilm formation, such as the operons responsible for curli and capsule synthesis and the M and O antigens, in addition to phospholipid synthesis. The genes in each experimental list can be in turn divided into two sets, depending on whether their level of expression increases or decreases upon a given perturbation. These sets are shown in Supplementary Table S5. The genes for motility and those for biofilm formation are

found for the most part on opposite sets. As a consequence, a given perturbation will affect the properties of most of the genes within this cluster by a change of gene expression in opposite directions for genes in the the two functional categories.

#### **E. Statistically significant periodicities emerge in the arrangement of nucleoid-perturbation sensitive genes along the genome.**

While the analysis described above identified specific large regions of high density of affected genes, previous studies have identified specific regular structures of the nucleoid that suggest a more global regulatory influence of nucleoid organization [37–39, 48]. We thus wanted to test the possibility that the genes that are sensitive to supercoiling variation and to deletion of Fis and H-NS may be organized in regularly spaced groups on the chromosome. We built the histogram of the position of the genes and the histogram of the distance between each pair of genes in the empirical lists of the chromosome.

The height of the spectral peaks for every periodicity in the empirical distributions was compared to the distribution of global maxima of a random null model shuffling the gene lists in order to discern statistically significant periodicities (see Methods and Supplementary Figures S8 and S9).

Supplementary Table S4 contains a synthetic summary of the periodicities found. A significant periodicity was found in the position distribution of the intra-strain WT list with period length of 352 Kb and a  $P$ -value  $< 0.04$ ; a similar periodicity was found also in the distance distribution with a period of 328 Kb ( $P < 0.01$ ). Another significant periodicity emerges in the  $\Delta$ Fis data set, with period length of 101 Kb ( $P < 0.01$ ); this periodicity was also confirmed by a similar signal in the distance distribution at about 98 Kb. The  $\Delta$ H-NS set shows a periodicity ( $P < 0.05$ ) appearing in the distance distribution at 20 Kb (which is below the resolution of the density histogram). In the WT- $\Delta$ H-NS(low  $-\sigma$ ) two periodicities emerge at 385 and 660 Kb ( $P < 0.01$ ). Both of them were confirmed in the distance distribution with a period of 331 and 589 Kb ( $P < 0.01$ ). A highly significant peak also emerges at the very large scale of 2.3 Mb, which is a sign of a genome wide asymmetry that confirms the results of the cluster analysis. A periodicity of 100 Kb also exists only in the distance distribution ( $P < 0.05$ ).

In the WT- $\Delta$ H-NS(high  $-\sigma$ ) list, two periodicities were found at 385 and 675 Kb ( $P < 0.01$ ). Both of them were confirmed in the distance distribution with periodicity of 370 and 660 Kb ( $P < 0.01$ ). Two periodicities at 22Kb and 100Kb were also found only in the distance distribution ( $P < 0.05$ ), while on the position distribution there is a non significant local maximum at 100Kb. No significant periodicity was detected in either the WT- $\Delta$ Fis(low  $-\sigma$ ) and WT- $\Delta$ Fis(high  $-\sigma$ ) empirical lists. It is worthwhile noticing that the periods detected in the distance distribution are systematically smaller than periods detected in the



density. However, the discrepancy is relatively small ( $< 10\%$ ) and always smaller than the bin-size of the density histogram.

In synthesis, we found the following significant periodicities, reported in supplementary table S4: one of  $20 \pm 36\text{Kb}$ , for  $\Delta\text{H-NS}$  and  $\text{WT-}\Delta\text{H-NS}$  (high  $-\sigma$ ), that could be comparable to the length of supercoiling domains [23], and one at  $100 \pm 36\text{Kb}$ , the same length of the solenoidal signal found by Wright and Kepes [39]. In addition, a periodicity around  $360 \pm 36\text{Kb}$ , which might be related to macrodomain size, appears under perturbation by both H-NS deletion and changes in supercoiling. The compatibility threshold of 36 Kb was set to twice the bin-size of the density distribution.

## Discussion

*Efficient detection of linear aggregation.* The large amount of high-throughput data being generated regarding genome organization and transcription requires the development of efficient approaches that are able to integrate different data sources. We developed a novel strategy to quantify the linear aggregation along the genome of different gene lists. This technique has the two main advantages of considering linear aggregation at all scales, and of being able to assign statistical confidence to the presence of gene clusters at different scales by comparing empirical data with suitable null models. We applied this method to multiple sets of experiments related to nucleoid protein binding and to the global transcriptional response to nucleoid perturbation, with a focus on the two nucleoid-shaping proteins Fis and H-NS.

*Clusters of contiguous genes responding transcriptionally to nucleoid perturbations appear to follow the macrodomain structure of the genome.* The results of the analysis confirm that the transcriptional response to nucleoid perturbations in the form of Fis/H-NS deletion and changes in the average level of supercoiling is highly non uniform along the genome [31], and reflected the results obtained from the analysis of binding profiles (see below). All the data analyzed, coming from independent sources [30–32], show multiple significant clusters whose arrangement is highly correlated with the probed spatial structure of the chromosome, and specifically with macrodomains [10, 12, 14, 25, 49]. Macrodomains have a well-defined spatial arrangement and localization in the cell both during chromosome segregation and during interphase, and preserve the linear order of genes along the genome [11, 13, 16, 49–52]. At larger scales, generally the clusters appear to overlap well with macrodomains, while at smaller scales they preferentially localize towards the edges of macrodomains or in nonstructured regions. This is particularly evident for the data producing clusters in the Ter region. These clusters also superimpose well with the segments of coherence between gene expression and codon bias [37]. Thus, we conclude that this evidence supports a tight link between large-scale transcription programs of the cell and the spatial organization of the genome

as a nucleoprotein-polymer complex [53].

Specifically, Fis and H-NS are known to be important protein factors for the shaping of the nucleoid [3, 6]. Fis is believed to create and isolate supercoiling domains by bridging two distant DNA regions, and is generally associated with positive transcriptional control. H-NS forms stable oligomers that bridge two DNA helices, stabilizing a plectoneme, and thus possibly inhibiting transcription [9, 54]. It is worthwhile noting that in the nucleoid perturbation experiments considered here, the clusters emerging from changing the supercoiling background and those that emerge under H-NS deletion are very similar, which suggests that the effects of these two different perturbations on the nucleoid might be related. A similar clustering behavior has recently been reported for the transcriptional response to deletions of the nucleoid protein Hu [55]. In this study it was found that the frequency of genes influenced by the absence of Hu correlates with the macrodomain organization of the nucleoid. The genes upregulated in the absence of Hu are found for the most part in the Ori macrodomain extending to the nearby nonstructured regions, while the genes downregulated in these conditions are found with higher frequency in the Ter and Right macrodomains. In addition the pattern of transcription upregulation in the Hu mutant mirrors the density of gyrase sites along the chromosome, pointing to a specific role of Hu in maintaining the supercoiling homeostasis in the rRNA-rich Ori macrodomain. On the other hand, the genes in the Ter macrodomain appear to be more sensitive to global changes in supercoiling and to regulation by Fis and H-NS in mid exponential phase (when rRNA expression is excluded). However, the Hu regulon does not show significant overlap with the Fis and H-NS regulons and with the genes influenced by supercoiling [30], only a small subset of genes are found to be co-regulated [56].

*Clusters of nucleoid-shaping protein binding spatially correlate with nucleoid perturbations.* The same clustering analysis applied to the binding of Fis and H-NS from ChIP-chip data [27, 28, 57] reveals clusters that correspond very well with those emerging from the transcriptomics data sets. We can also report that our preliminary survey of very recent ChIP-seq data for the same proteins also agrees with these findings [58]. This confirms that the two proteins also have a direct role in physically shaping the region of the nucleoid that responds to their action. More specifically, deletion of H-NS influences the expression of the genes in the cluster at 1.1Mb (24 centisomes), which overlaps with the cluster of Fis binding from the ChIP-Chip dataset, pointing to a tight link between the activity of these two proteins. Moreover the cluster at 2Mb (43 centisomes) is also enriched for heEPODS, high expression extended protein occupancy domains [29].

It is important to note that while the two transcriptomics datasets and the EPOD results were obtained from cells growing in rich media (LB or YT), the ChIP-chip data from the other two experiments was obtained from cells growing in minimal media (M9 plus glucose or fructose), with the exception of the

Oshima data, which refer to mid-exponential growth phase in LB medium. Most data relate to cells in mid exponential phase, which suggests that the coherent results between binding patterns and transcriptional response to perturbation might correspond to growth-phase specific features. In addition, some variation may also arise from the loose definition of “mid exponential phase”, determining when the cells are harvested after dilution in fresh medium. The agreement of these different datasets indicates that the positioning of the clusters is robust within this range of experimental conditions. The dataset that addresses directly the changes in gene expression as a function of growth phase, shows that the clusters reflect changes in cellular metabolism (see Supplementary Figure S2). In the future, we expect that further studies will directly probe the role of nucleoid structure and organization in response to changes of both growth rate and growth phase.

*Coherent periodicity signals emerge from both nucleoid protein binding and transcriptional response to nucleoid perturbations.* We also found significant evidence for periodic arrangement of the nucleoid perturbation sensitive genes. Some of these periodicities correspond to characteristic lengths that can be associated to supercoil domains, the  $\sim 20\text{Kb}$  branched structure of genomic plectonemes [23] or the previously observed 100Kb periodicity of evolutionarily conserved gene sets [38]. Notably, as in the clustering analysis, the periodicities emerging from supercoil perturbation also correspond to those related to H-NS deletion. Evidence for spatial organization of genes along the chromosome has already been presented for *E. coli K12* [38, 39, 48], and models that could explain it have been formulated in the form of the so-called “rosette model” [59], and the “solenoid model” [39, 40]. In the case of our data the question remains open regarding whether the periodic signal is simply related to the presence of clusters. This is technically difficult to test, as it would require a null model that randomizes a list by keeping its linear aggregation properties constant. It is possible that newly developed techniques are effective in bypassing this problem [60].

*The two main clusters at the edges of the Ter macrodomain include the whole flagella regulon and key regulators of biofilm formation.* We will now focus on the possible functional aspects of the clusters. This analysis has identified two clusters of genes on either side of the Ter macrodomain (Cluster 1 and 4) whose expression is affected by deletion of either Fis or H-NS and upon changes in negative supercoiling [30–32], in addition these clusters superimpose with those obtained from the analysis of Fis and H-NS binding obtained by ChIP-chip [27, 61]. The list of genes in these two clusters include all the operons for flagellar proteins and several genes required for cell adhesion and the formation of biofilms. The expression of flagella is induced when the bacteria need to swim either away from a stress or towards a richer nutrient environment. Swimming is also necessary for the first steps of biofilms formation leading to reversible attachment. However, flagella synthesis is soon shut down as the biofilm structure begins to form (reviewed in [62, 63]). A similar exclusive gene expression program takes place when the cells transit from

exponential growth into stationary phase. For example, below 30 °C the genes needed for the synthesis of curli fimbriae are induced, while expression of the flagella is repressed via a regulatory network where the second messenger c-di-GMP is important [64].

Expression of flagella takes place in a sequential pattern corresponding to the order of assembly of the different protein components [65, 66]. The flagellar expression cascade is controlled by a master regulator FlhDC, and FliA, the flagella-specific sigma factor. This regulatory network also includes post-transcriptional and post-translational regulation and feedback control [67, 68].

*Symmetric clustered organization of the flagella regulon.* The organization of the flagellar regulon in the two nucleoid-related clusters identified here could suggest a differential regulation of these two sets of genes. However, the sequential order of expression is not reflected in their linear organization along the chromosome (Supplementary Table S5). On the other hand, their position on opposite sides of the two replicores suggests that it may bring an advantage to replicate these two clusters roughly simultaneously instead of sequentially, in order to maintain the relative proportions of the flagellar proteins.

Moreover, the two sides of the regulon would attain on average equal accumulated supercoiling from replication rounds, which would make (in absence of stable topological barriers) symmetrically placed genes on different replicores sense similar physical cues. This may confer a specific sensitivity of these regions to changes in supercoiling and nucleoid protein abundance that play a role in differential expression under different kinds of stresses.

Another interesting question is whether this symmetry is common across bacterial species. Certainly this is true for close species such as *Salmonella*. On the other hand, there are indications that this symmetric arrangement might be a general principle. Studies of bacterial comparative genomics [38] show a tendency of cofunctional genes to be placed symmetrically with respect to replication origins. Other studies [69, 70] uncovered evidence for preferred symmetric chromosomal inversions around the replication origin in evolving bacteria, which would preserve a symmetric arrangement of genes.

*Are the flagella regulon clusters part of a hyperstructure?* At the same time, it is plausible that the two clusters are in contact or found near each other in the cytoplasm due to the compaction of the Ter macrodomain [71]. One can speculate that these clusters are part of a larger structure that is co-localized in three-dimensional space, and that both spatial aspects and physico-chemical ones contribute to its function. Following the example of the eukaryotic field, these spatial relationships could emerge from both computational [72] and experimental studies [73]. The preference of a possible structure that colocalizes genes to be mirror-symmetric can be argued by the fact that it would be disrupted only once per replication round by advancing replication forks.

*Direct and indirect nucleoid-based regulation of the flagella-regulon clusters.* As described above, our analysis has identified these clusters because of the high density in genes whose expression is affected by specific nucleoid perturbations and/or high density of nucleoid protein binding sites. Supercoiling, Fis and H-NS are known regulators of flagellar expression in several organisms [44–47]. It is useful to discuss the effects that these parameters may have on the expression of the global regulators or directly on the different genes found downstream in the regulatory network.

H-NS can influence the expression of the FlhDC transcription factor both directly and indirectly through the regulation of expression of the HdfR and RcsAB transcription factors [46, 75, 82] resulting in a feed forward loop mode of regulation (Figure 3). RcsAB also represses the curli fimbriae operon in Cluster 4 (csgDEFG, csgBAC) and positively regulates the expression of the colanic acid operon in Cluster 3 (20 genes). Colanic acid is an important component of the capsule necessary for mature biofilm formation [63]. The gene for RcsA is adjacent to one of the flagellar regulon in Cluster 2 and is induced in the strain lacking H-NS (Supplementary Table S6), while the gene for RcsB, which is also involved in the regulation of acid stress response, is found in the Left macrodomain and is independently regulated. As possible evidence for direct regulation by H-NS, a cluster of H-NS binding is observed in the ChIP-chip data for Cluster 1 but not for Cluster 4 (Table S1), nevertheless some predicted H-NS sites are also found near or at three of the operons in Cluster 4: csgDEFG, flgMN and flgBCDEFGHIJ (Supplementary Table S6) [33].

This direct regulation by H-NS can in turn be differentiated into two nonexclusive mechanisms of transcription regulation: H-NS can directly influence the binding of RNA polymerase but it can also result in a change in DNA topology by the formation of oligomeric structures [54]. For example, the flagellar genes are in general activated by the presence of H-NS independently of the supercoiling state of the DNA, in part probably because of the induction of the *fliA* gene, however the ones in Cluster 4, including the FlgM anti-sigma factor, are also induced by a change in topology (Supplementary Table S6). On the other hand, the *flhD* gene is found on all the hyp lists, confirming that it is activated by an increase in negative supercoiling, independently of the presence of Fis or H-NS, in accordance with experimental *in vitro* and *in vivo* observations [83].

As already mentioned for the regulation by RcsAB, in addition to the flagellar operons, Cluster 1 and 4 also contain several other genes involved in biofilm formation and maturation that are influenced by the different perturbations to the nucleoid, as shown in Supplementary Table S6. These include the genes coding for the O-antigen, the M-antigen, colanic acid, capsule formation, curli synthesis, antigen 43 and several transcription factors that can affect expression of genes outside of these clusters (Figure 3), such as RcsA, CsgD, SdiA and UvrY [63]. The change in the local DNA structure and topology affects these two classes of genes in opposite ways thus contributing to the transition from a motility to an adherence

phenotype (Supplementary Table S5).

While the role of H-NS in the regulation of these pathways is well known, the role of Fis is still less well-defined. A large set of flagellar genes is activated by Fis both under high and low supercoiling conditions, mostly those found in Cluster 1, while the expression of *csgA* is repressed by Fis at low supercoiling as reported by [45, 77] (Supplementary Table S6). In addition, Fis seems to mediate the supercoiling dependence of *flhC* and *rcaA* expression, the first being in the  $\Delta$ Fis hyp and the second in the  $\Delta$ Fis rel list. These two proteins play opposite roles on flagellar synthesis pathway (Figure 3).

Finally, Cluster 6 in the Ori macrodomain corresponds to the chromosomal *waa* region containing the operons for lipopolysaccharide (LPS) synthesis necessary for biofilms formation [63]. The genes found in this cluster respond to changes in supercoiling in the absence of Fis, overlapping with a cluster of H-NS binding sites as shown by ChIP-chip analysis, consistent with the presence of several predicted H-NS sites according to Lang et al [33]. The chromosomal map of the known genes involved in synthesis and regulation of flagella, chemotaxis and the different stages of biofilm formation reveals a preferential localization in the Ori and Ter macrodomains (Figure 3).

To conclude, we believe that this study shows the power of the integrated analysis of distinct datasets in the context of the role played by the nucleoid in transcription. In the future, in order to more easily integrate datasets from different sources, it will be necessary to start a common effort towards the construction of larger comprehensive databases and consortia collecting, sharing and analyzing data obtained with different high- and low- throughput techniques.

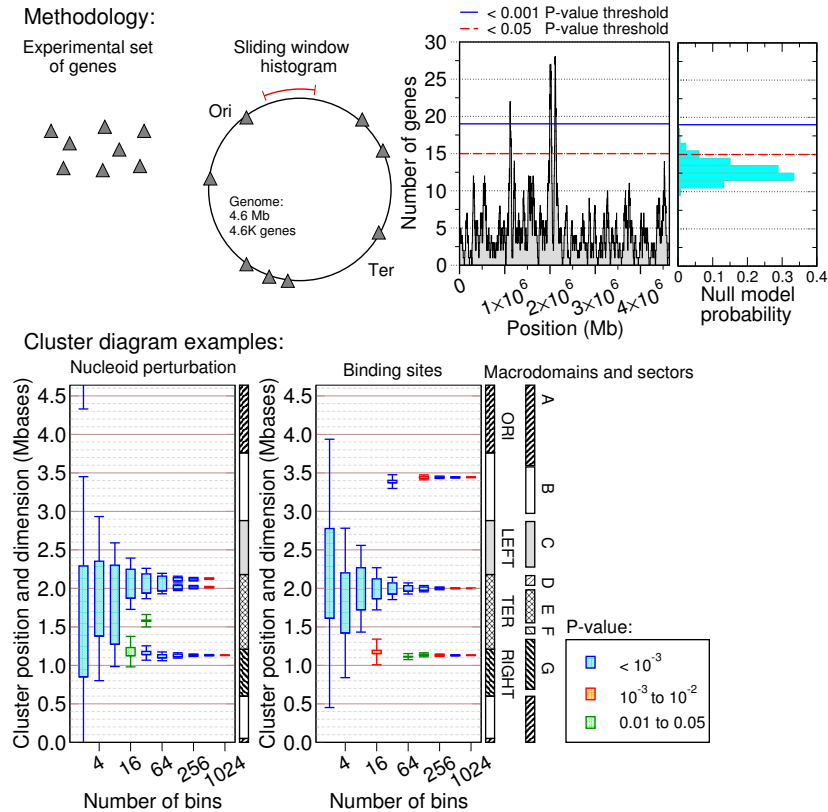


**Figure 1** Procedure followed to detect one-dimensional aggregation of genes in the lists. Top panel: A sliding-window density histogram associates to every coordinate on the circular genome the number of genes in the empirical list in an interval surrounding the point and spanning a fixed bin-size. As an example, the density histogram of the WT- $\Delta$ H-NS(low  $-\sigma$ ) list at bin-size  $b_s = L/256$  is shown; the density of each position is compared with the  $P$ -value thresholds from the null model (Methods) in order to obtain the significant positions, which are in turn merged with a compatibility threshold of size  $b_s$  in order to define the clusters. Bottom panel: example of cluster diagram for the WT- $\Delta$ H-NS(low  $-\sigma$ ) transcriptomics data, and the FISbind(Grainger) protein binding data. The  $y$ -axis is the genome coordinate. The plot shows the clusters discovered at different scales as a function of the number of bins  $L/b_s$  ( $x$ -axis). The box indicates the position of the peak while the whiskers span the maximal extension of the clusters. Both cluster diagrams give clusters that localize close to the edges of the Ter macrodomain at small scales ( $L/1024 \simeq 5Kb$  to  $L/16 \simeq 0.3Mb$ ), and cover the Ter or the Ter+Left region at larger scales ( $L/4 \simeq 1.2Mb$  or more). The binding data have a cluster in the nonstructured Left region appearing only at small scales ( $L/16$  or less).

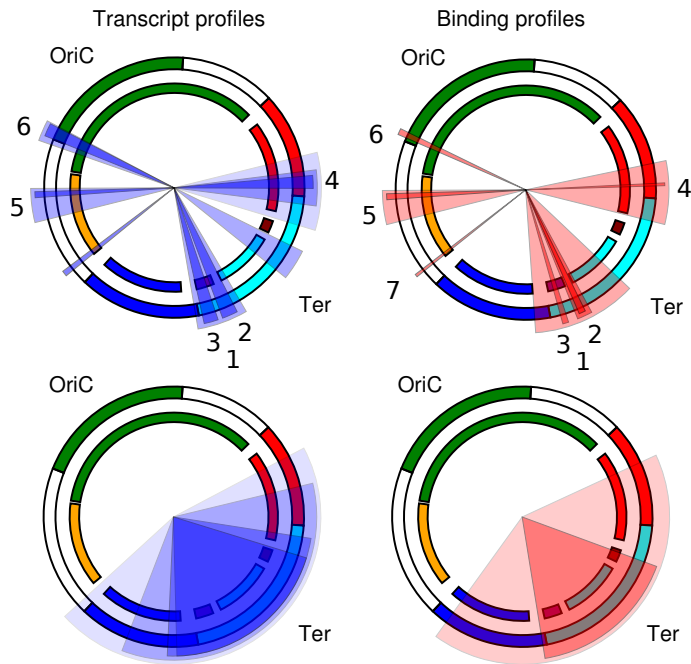


**Figure 2** Graphical representation of the most significant clusters found for nucleoid perturbation transcriptomics data (left) and for data of direct binding of Fis and H-NS (right). The clusters found are represented by colored wedges with transparency increasing with size. The clusters found at large observation scales ( $L/8 \simeq 0.6Mb$  or more) are shown separately in the lower panels. In the drawings, the outer colored circle represents macrodomains while inner colored circle contains the chromosome sectors defined by Mathelier and Carbone [37]. The numbering of the small clusters is described in Supplementary Table S1. Note the compatibility of the clusters found with the edges of the Ter and Ori macrodomains at small scales and with different segments of the Ter region at larger scales.



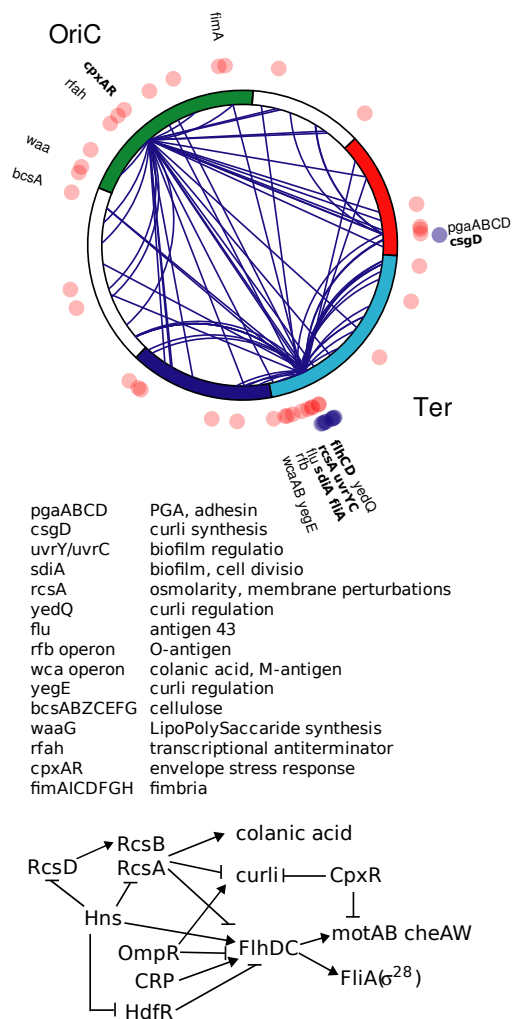


**Figure 3** (top panel) The main genes for flagella, chemotaxis and biofilm formation are partitioned between the Ori and the Ter macrodomains and particularly within Cluster 1 and 4 obtained from the analysis (Figure 2). The blue dots correspond to the flagellar and chemotaxis genes. The red dots correspond to the genes related to biofilm formation (increased color intensity results from presence of closely spaced genes). The unlabeled red dots correspond to various cryptic fimbriae and adhesins operons, according to the lists in Supplementary Table S6. The gene names in bold correspond to transcription factors, and the blue lines to interactions from these transcription factors to their targets (RegulonDB). (bottom panel) Direct and indirect regulation of flagellar and curli expression, see refs. [46, 63, 74–80]. For additional levels of regulation mediated by c-di-GMP see [64, 74, 81].

## II. METHODS

### A. Microarray data of Fis, H-NS, and supercoil sensitive genes.

We used microarray data from Blot *et al.* [30], where the wild type level of gene expression is measured (from cells growing in rich media) relative to genetically engineered *E. coli* LZ41 and LZ54 strains containing drug-resistant topoisomerase gene alleles to inhibit DNA gyrase or topoisomerase IV activity selectively [84] and thereby inducing negative supercoil relaxation ( $-\sigma < 0.033$  on average, as measured on plasmids) or increase ( $-\sigma > 0.08$  on average, as measured on plasmids). In addition, these strains were crossed with the knockouts  $\Delta$ Fis and  $\Delta$ H-NS in order to determine the coupling of the effect of a specific nucleoid protein with a specific level of supercoiling. These experiments define seven sets of nucleoid-perturbation sensitive genes relative to pairs of conditions compared. The so-called “intra-strain” sets include the genes that change significantly their expression when the negative superhelical density  $\sigma$  varies in a fixed genetic background. The “inter-strain” sets include the genes that change significantly their expression at a fixed average supercoiling background ( $-\sigma < 0.033$  or  $-\sigma > 0.08$ ) comparing the transcript profiles of the wild-type and knockout mutant.

In the text we refer to intra-strain lists by the name of the relative mutant, WT,  $\Delta$ Fis and  $\Delta$ H-NS, and to inter-strain lists by the names of the two mutants compared, with a suffix indicating the supercoiling condition, WT- $\Delta$ Fis (high or low  $-\sigma$ ), WT- $\Delta$ H-NS (high or low  $-\sigma$ ). Supplementary Figure SM1 summarizes both the experimental sets and the gene lists.

We also considered microarray data on a  $\Delta$ Fis strain in different growth phases (early, mid-, late-exponential and stationary, in rich media) from both Bradley *et al.* [32] and Blot *et al.* [30] datasets. The lists of genes significantly changing their expression with respect to wild type are referred to by the names of the two mutants compared with a suffix indicating the growth phase, WT- $\Delta$ Fis (early/mid/late/stat phase) for Bradley data and WT- $\Delta$ Fis/H-NS (LS or late stationary phase/ME or mid-exponential phase/TS or transition phase) for data from Blot *et al.*.

### B. Transcription network.

The transcription network interactions were compiled from the RegulonDB 6.0 database [8], which contains a concise representation of the information available from the literature about transcriptional regulation of all genes in *E. coli*. Interactions inferred purely from microarrays were filtered out in order to decrease the contribution of indirect effects. Of 4552 genes in *E. coli*, 1524 genes are in the unfiltered network in

RegulonDB, 1372 are in the filtered network and of these 166 and 140 respectively are transcription factors, out of the 286 genes functionally annotated as transcription factors in *E. coli* by Gene Ontology [85, 86].

### C. ChIP-chip binding profiles and protein occupancy data.

Binding sites from ChIP-chip data of H-NS and Fis proteins along the *E. coli* genome *in vivo* were obtained from Grainger *et al.* [27]. These sets are referred to as FISbind(Grainger), HNSbind(Grainger) in the text. As a comparison, we also considered the list of Fis binding sites obtained by high-density ChIP-chip by Cho *et al.* [28], identifying 894 Fis-associated binding regions (compared to the 224 regions found by Grainger *et al.*), referred to as FISbind(Cho), and the list of H-NS binding data from Oshima *et al.* [57], HNSbind(Oshima). We also considered data from RegulonDB for Fis and H-NS binding sites, referred to as FISbind(RegulonDB) and HNSbind(RegulonDB) in the text. In order to quickly compare the overlap between RegulonDB target genes and Fis and H-NS ChIP-chip data sets we have carried out a hypergeometric test with results reported in Supplementary Table SM1. Both ChIP-chip data sets refer to cells grown in minimal media.

Finally, the data from Vora *et al.* (ref. [29]) was considered. In this study the amount of total protein-DNA interactions at a specific locus *in vivo* was measured (from cells grown in rich media) by a modified large-scale ChIP assay measuring generic protein occupancy along the genome (termed *in vivo* protein occupancy display, IPOD). Specifically, we examined the ( $> 1$  Kb) protein occupancy domains (EPODs), divided by the authors into two populations by their median expression level (121 domains in the highly expressed class, heEPODs, and 151 in the transcriptionally silent class, tsEPODs).

### D. Statistical analysis of spatial clusters.

We developed a statistical method for identifying clusters of genes in the lists along the genomic coordinate. This method considers the density of genes at different scales on the genome, and compares empirical data with results from random null models. In order to avoid spurious effects of binning, for each gene list a density histogram was made by using a sliding window with a given bin-size  $b_s$  as exemplified in Figure 1. The resulting plot of the averaged density of genes for every point of the circular chromosome was considered at different observation scales of the genome, i.e. at different bin sizes of length  $b_s \in \{L/2, L/4, \dots, L/2^n\}$  where  $L$  is the length of the chromosome. We chose  $n = 10$ , as  $b_s < L/1024$  is the scale of the typical gene length.

Density peaks with a significantly high number of genes (see also Figure 1) were identified by comparing

empirical data with 10000 realizations of a null model. For every bin size, the null model considers the density histogram from a random list of the same length of the empirical one. The number of genes for every bin in the empirical histogram was compared to the distribution of global maxima of the null model, obtaining a  $P$ -value for the value of the empirical histogram for each bin. This procedure enables to extract a list of statistically significant ( $P < 0.05$ ) bin positions. For each bin-size (or observation scale), clusters were defined as connected intervals containing a significantly high proportion of the genes in the list. To each cluster, we assigned the lowest  $P$ -value among the merged bins.

#### **E. Macrodomains and chromosomal sectors.**

The location of the chromosomal macrodomains were extracted from [10, 12, 49], and considered together with the chromosomal sectors of ref. [37] where codon bias indices positively correlate with gene expression. The exact coordinates used here are presented in Supplementary Table SM2

#### **F. Periodicity analysis.**

Periodic signals in the position of genes of a given list were derived from both the density (histogram of the start position of each gene) and the histogram of the shortest distances along the genome between any gene pair. We computed the discrete Fast Fourier transform of this function. For every frequency  $\nu$ , the spectra of the Fourier transform is proportional to the strength of the periodic signal of period  $\lambda = 1/\nu$ , while the complex phase  $\theta$  is proportional to a shift of the periodic distribution  $\tau = \theta\lambda/2\pi$  with respect to the sinusoidal periodic distribution of that period. Note that the resolution of this analysis is limited to a few bin sizes, so that since the distance distribution between gene pairs contains more data points, it allows to probe more effectively smaller length scales. Being  $L$  the number of bases in the chromosome (the maximal distances is  $L/2$ ) we used a bin-size of  $L/256$  bases for the position histogram and a bin-size of  $L/2048$  bases for the distance histogram.

Peaks exhibited by empirical data were scored with the same null model used for the cluster analysis, i.e. randomized lists of genes conserving the length of the empirical list. Given an empirical list, we generated 500 random lists of the same length. The lower sampling compared to the 10000 random lists generated for the clustering is due to the fact that the pair distance distribution requires the storage and elaboration of  $n^2$  data points instead of  $n$ , which causes a consequent increase of computing time. The height of the spectral peaks for every periodicity in the empirical distributions was compared to the distribution of global maxima of the null model (regardless of their position in the spectrum) as exemplified in Supplementary Figure S8,

a periodicity with a  $P$ -value  $< 0.05$  was considered to be statistically significant.

### G. Functional annotations.

Functional annotations were downloaded from the MultiFun web site <http://genprotec.mbl.edu/> [43]. Gene sets belonging to clusters and effective networks were probed for enrichment of functional annotations by hypergeometric testing.  $P$ -values lower than  $10^{-3}$  were considered significant.

### Acknowledgments

The authors acknowledge support from the Human Frontier Science Program Organization (Grant RGY0069/2009-C). We are also very grateful to A. Travers, G. Muskhelishvili, and V.G. Benza for critical reading of this manuscript and to O. Espeli, A. Carbone, I. Junier and A. Mathelier for useful discussions.

- 
- [1] B. Alberts, D. Bray, J. Lewis, M. Raff, K. Roberts and J. D. Watson, *Molecular Biology of the Cell*, Garland, London, New York, 2003.
  - [2] I. Cases, V. de Lorenzo and C. A. Ouzounis, *Trends Microbiol*, 2003, **11**, 248–53.
  - [3] S. C. Dillon and C. J. Dorman, *Nat Rev Microbiol*, 2010, **8**, 185–195.
  - [4] A. Travers and G. Muskhelishvili, *Curr Opin Genet Dev*, 2005, **15**, 507–14.
  - [5] D. J. Jin and J. E. Cabrera, *J Struct Biol*, 2006, **156**, 284–91.
  - [6] M. S. Luijsterburg, M. C. Noom, G. J. Wuite and R. T. Dame, *J Struct Biol*, 2006, **156**, 262–72.
  - [7] M. M. Babu, N. M. Luscombe, L. Aravind, M. Gerstein and S. A. Teichmann, *Curr Opin Struct Biol*, 2004, **14**, 283–91.
  - [8] S. Gama-Castro, V. Jimenez-Jacinto, M. Peralta-Gil, A. Santos-Zavaleta, M. I. Penaloza-Spinola, B. Contreras-Moreira, J. Segura-Salazar, L. Muniz-Rascado, I. Martinez-Flores, H. Salgado, C. Bonavides-Martinez, C. Abreu-Goodger, C. Rodriguez-Penagos, J. Miranda-Rios, E. Morett, E. Merino, A. M. Huerta, L. Trevino-Quintanilla and J. Collado-Vides, *Nucleic Acids Res*, 2008, **36**, D120–4.
  - [9] R. T. Dame, M. S. Luijsterburg, E. Krin, P. N. Bertin, R. Wagner and G. J. Wuite, *J Bacteriol*, 2005, **187**, 1845–8.
  - [10] M. Valens, S. Penaud, M. Rossignol, F. Cornet and F. Boccard, *EMBO J*, 2004, **23**, 4330–41.
  - [11] E. Esnault, M. Valens, O. Espéli and F. Boccard, *PLoS Genet*, 2007, **3**, e226.
  - [12] F. Boccard, E. Esnault and M. Valens, *Molecular Microbiology*, 2005, **57(1)**, 9–16.

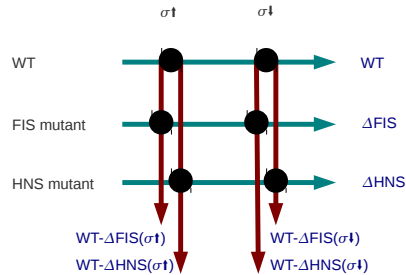
- [13] O. Espéli, R. Mercier and F. Boccard, *Mol Microbiol*, 2008, **68**, 1418–27.
- [14] P. A. Wiggins, K. C. Cheverallsa, J. S. Martina, R. Lintnera and J. Kondev, *PNAS Early Edition*, 2010, [www.pnas.org/cgi/doi/10.1073/pnas.0912062107](http://www.pnas.org/cgi/doi/10.1073/pnas.0912062107).
- [15] X. Wang, R. Reyes-Lamothe and D. Sherratt, *Biochem Soc Trans*, 2008, **36**, 749–53.
- [16] X. Wang, X. Liu, C. Possoz and D. J. Sherratt, *Genes Dev*, 2006, **20**, 1727–31.
- [17] S. Cunha, C. L. Woldringh and T. Odijk, *J Struct Biol*, 2005, **150**, 226–32.
- [18] S. Cunha, T. Odijk, E. Suleymanoglu and C. L. Woldringh, *Biochimie*, 2001, **83**, 149–54.
- [19] S. B. Zimmerman, *J Struct Biol*, 2006, **156**, 255–61.
- [20] J. E. Cabrera and D. J. Jin, *J Bacteriol*, 2006, **188**, 4007–14.
- [21] M. Liu, T. Durfee, J. E. Cabrera, K. Zhao, D. J. Jin and F. R. Blattner, *J Biol Chem*, 2005, **280**, 15921–7.
- [22] J. E. Cabrera and D. J. Jin, *Mol Microbiol*, 2003, **50**, 1493–505.
- [23] L. Postow, C. Hardy, J. Arsuaga and N. Cozzarelli, *Genes Dev*, 2004, **18**, 1766–79.
- [24] B. J. Peter, J. Arsuaga, A. M. Breier, A. B. Khodursky, P. O. Brown and N. R. Cozzarelli, *Genome Biol*, 2004, **5(11)**, R87.
- [25] L. Moulin, A. Rahmouni and F. Boccard, *Mol Microbiol*, 2005, **55**, 601–10.
- [26] J. T. Wade, K. Struhl, S. J. Busby and D. C. Grainger, *Mol Microbiol*, 2007, **65**, 21–6.
- [27] D. C. Grainger, D. Hurd, M. D. Goldberg and S. J. W. Busby, *Nucleic Acids Research*, 2006, **34**, 4642–4652.
- [28] B. K. Cho, E. M. Knight, C. L. Barret and et al., *Genome Res.*, 2008, **18**, 900–910.
- [29] T. Vora, A. K. Hottes and S. Tavazoie, *Molecular Cell*, 2009, **35**, 247–253.
- [30] N. Blot, R. Mavathur, M. Geertz, A. Travers and G. Muskhelishvili, *Embo Rep.*, 2006, **7**, 710–715.
- [31] C. Marr, M. Geertz, M. Hütt and G. Muskhelishvili, *BMC Syst Biol*, 2008, **2**, 18.
- [32] M. D. Bradley, M. B. Beach, A. P. J. de Koning, T. S. Pratt and R. Osuna, *Microbiology*, 2007, **153**, 2922–2940.
- [33] B. Lang, N. Blot, E. Bouffartigues, M. Buckle, M. Geertz, C. O. Gualerzi, R. Mavathur, G. Muskhelishvili, C. L. Pon, S. Rimsky, S. Stella, M. M. Babu and A. Travers, *Nucleic Acids Res*, 2007, **35**, 6330–7.
- [34] P. N. Hengen, S. L. Bartram, L. E. Stewart and T. D. Schneider, *Nucleic Acids Res*, 1997, **25**, 4994–5002.
- [35] P. B. Warren and P. R. ten Wolde, *J Mol Biol*, 2004, **342**, 1379–90.
- [36] N. Sonnenschein, M.-T. Hütt, H. Stoyan and D. Stoyan, *BMC Syst Biol*, 2009, **3**, 119.
- [37] A. Mathelier and A. Carbone, *Mol Syst Biol*, 2010, **6**, 366.
- [38] M. A. Wright, P. Kharchenko, G. M. Church and D. Segre, *Proc Natl Acad Sci U S A*, 2007, **104**, 10559–64.
- [39] F. Képès, *J Mol Biol*, 2004, **340**, 957–64.
- [40] F. Képès and C. Valliant, *ComplexUs*, 2003, **1**, 171–180.

- [41] C. A. Ball, R. Osuna, K. C. Ferguson and R. C. Johnson, *J Bacteriol*, 1992, **174**, 8043–8056.
- [42] C. J. Dorman, *Nat Rev Microbiol*, 2004, **2**, 391–400.
- [43] M. H. Serres and M. Riley, *Microb Comp Genomics*, 2000, **5**, 205–222.
- [44] P. Bertin, E. Terao, E. H. Lee, P. Lejeune, C. Colson, A. Danchin and E. Collatz, *J Bacteriol*, 1994, **176**, 5537–5540.
- [45] A. Kelly, M. D. Goldberg, R. K. Carroll, V. Danino, J. C. D. Hinton and C. J. Dorman, *Microbiology*, 2004, **150**, 2037–2053.
- [46] M. Ko and C. Park, *J Bacteriol*, 2000, **182**, 4670–4672.
- [47] O. A. Soutourina and P. N. Bertin, *FEMS Microbiol Rev*, 2003, **27**, 505–523.
- [48] K. Jeong, J. Ahn and A. Khodursky, *Genome Biol*, 2004, **5**, R86.
- [49] O. Espéli and F. Boccard, *J Struct Biol*, 2006, **156**, 304–10.
- [50] E. P. Rocha, *Annu Rev Genet*, 2008.
- [51] H. J. Nielsen, Y. Li, B. Youngren, F. G. Hansen and S. Austin, *Mol Microbiol*, 2006, **61**, 383–93.
- [52] R. Reyes-Lamothe, X. Wang and D. Sherratt, *Trends Microbiol*, 2008, **16**, 238–45.
- [53] G. Muskhelishvili, P. Sobetzko, M. Geertz and M. Berger, *Mol Biosyst*, 2010, **6**, 662–676.
- [54] F. C. Fang and S. Rimsky, *Curr Opin Microbiol*, 2008, **11**, 113–120.
- [55] M. Berger, A. Farcas, M. Geertz, P. Zhelyazkova, K. Brix, A. Travers and G. Muskhelishvili, *EMBO Rep*, 2010, **11**, 59–64.
- [56] J. Oberto, S. Nabti, V. Jooste, H. Mignot and J. Rouviere-Yaniv, *PLoS One*, 2009, **4**, e4367.
- [57] T. Oshima, S. Ishikawa, K. Kurokawa, H. Aiba and N. Ogasawara, *DNA Res*, 2006, **13**, 141–153.
- [58] C. Kahramanoglou, A. S. N. Seshaseyee, A. I. P. D. Ibberson, S. Schmidt, J. Zimmermann, V. Benes, G. M. Fraser and N. M. Luscombe, *Nucleic Acids Res*, 2010.
- [59] P. R. Cook, *Nature Genetics*, 2002, **32**, 347–352.
- [60] I. Junier, J. Herisson and F. Kepes, *Algorithms Mol Biol*, 2010, **5**, 31.
- [61] B. K. Cho and B. Palsson, *Molecular Cell*, 2009, **35**, 255–256.
- [62] B. M. Prüss, C. Besemann, A. Denton and A. J. Wolfe, *J Bacteriol*, 2006, **188**, 3731–3739.
- [63] C. Beloin, A. Roux and J. M. Ghigo, *Curr Top Microbiol Immunol*, 2008, **322**, 249–289.
- [64] H. Weber, C. Pesavento, A. Possling, G. Tischendorf and R. Hengge, *Mol Microbiol*, 2006, **62**, 1014–1034.
- [65] G. S. Chilcott and K. T. Hughes, *Microbiol Mol Biol Rev*, 2000, **64**, 694–708.
- [66] S. Kalir, J. McClure, K. Pabbaraju, C. Southward, M. Ronen, S. Leibler, M. G. Surette and U. Alon, *Science*, 2001, **292**, 2080–2083.

- [67] S. Kalir, S. Mangan and U. Alon, *Mol Syst Biol*, 2005, **1**, 2005.0006.
- [68] T. G. Smith and T. R. Hoover, *Adv Appl Microbiol*, 2009, **67**, 257–295.
- [69] A. E. Darling, I. Miklós and M. A. Ragan, *PLoS Genet*, 2008, **4**, e1000128.
- [70] J. A. Eisen, J. F. Heidelberg, O. White and S. L. Salzberg, *Genome Biol*, 2000, **1**, RESEARCH0011.
- [71] R. Mercier, M.-A. Petit, S. Schbath, S. Robin, M. E. Karoui, F. Boccard and O. Espéli, *Cell*, 2008, **135**, 475–485.
- [72] S. C. Janga, J. Collado-Vides and M. M. Babu, *PNAS*, 2008, **105**, 15761–15766.
- [73] Z. Duan, M. Andronescu, K. Schutz, S. McIlwain, Y. J. Kim, C. Lee, J. Shendure, S. Fields, C. A. Blau and W. S. Noble, *Nature*, 2010, **465**, 363–367.
- [74] R. Hengge, *Nat Rev Microbiol*, 2009, **7**, 263–273.
- [75] E. Krin, A. Danchin and O. Soutourina, *Res Microbiol*, 2010, **161**, 363–371.
- [76] H. Ogasawara, K. Yamada, A. Kori, K. Yamamoto and A. Ishihama, *Microbiology*, 2010, **156**, 2470–2483.
- [77] Z. Saldana, J. Xicohtencatl-Cortes, F. Avelino, A. D. Phillips, J. B. Kaper, J. L. Puente and J. A. Giri $\frac{1}{2}$ n, *Environ Microbiol*, 2009, **11**, 992–1006.
- [78] X. Wang, J. F. Preston and T. Romeo, *J Bacteriol*, 2004, **186**, 2724–2734.
- [79] C.-G. Korea, R. Badouraly, M.-C. Prevost, J.-M. Ghigo and C. Beloin, *Environ Microbiol*, 2010, **12**, 1957–1977.
- [80] C. Prigent-Combaret, E. Brombacher, O. Vidal, A. Ambert, P. Lejeune, P. Landini and C. Dorel, *J Bacteriol*, 2001, **183**, 7213–7223.
- [81] C. Pesavento and R. Hengge, *Curr Opin Microbiol*, 2009, **12**, 170–176.
- [82] O. Soutourina, A. Kolb, E. Krin, C. Laurent-Winter, S. Rimsky, A. Danchin and P. Bertin, *J Bacteriol*, 1999, **181**, 7500–7508.
- [83] O. A. Soutourina, E. Krin, C. Laurent-Winter, F. Hommais, A. Danchin and P. N. Bertin, *Microbiology*, 2002, **148**, 1543–1551.
- [84] E. L. Zechiedrich, A. B. Khodursky and N. R. Cozzarelli, *Genes Dev.*, 1997, **11**, 2580–2592.
- [85] I. M. Keseler, C. Bonavides-Martínez, J. Collado-Vides, S. Gama-Castro, R. P. Gunsalus, D. A. Johnson, M. Krummenacker, L. M. Nolan, S. M. Paley, I. T. Paulsen, M. Peralta-Gil, A. D. Santos-Zavaleta, A. G. Shearer and P. D. Karp, *Nucleic Acids Research*, 2009, **37**, 464–470.
- [86] M. Ashburner, C. A. Ball, J. A. Blake, D. Botstein, H. Butler, J. M. Cherry, A. P. Davis, K. Dolinski, S. S. Dwight, J. T. Eppig, M. A. Harris, D. P. Hill, L. Issel-Tarver, A. Kasarskis, S. Lewis, J. C. Matese, J. E. Richardson, M. Ringwald, G. M. Rubin and G. Sherlock, *Nature Genetics*, 2000, **25**, 25–29.



## Supplementary methods for Scolari *et al*



**Supplementary Methods Figure SM1** Summary of microarray data of Fis, H-NS, and supercoil sensitive genes.

		RegulonDB	Cho <i>et al</i>	Grainger <i>et al</i>			RegulonDB	Grainger <i>et al</i>
<b>(a)</b>	RegulonDB	200	58 ( $P = 10^{-4}$ )	11 ( $P = 0.26$ )	<b>(b)</b>	RegulonDB	71	1 ( $P = 0.44$ )
	Cho		894	71 ( $P = 10^{-9}$ )		Grainger		96
	Grainger			220				

**Supplementary Methods Table SM1** The table compares reported Fis **(a)** and H-NS **(b)** binding sites from different data sources. The table reports the number of genes in the overlap between the lists, and the  $P$ -value in parentheses.

		Macro-	Ori		Right		Ter		Left	
<b>(a)</b>	<b>domain:</b>		start	end	start	end	start	end	start	end
	Position ( <i>Mb</i> )		3.76	0.05	0.60	1.21	1.21	2.18	2.18	2.88

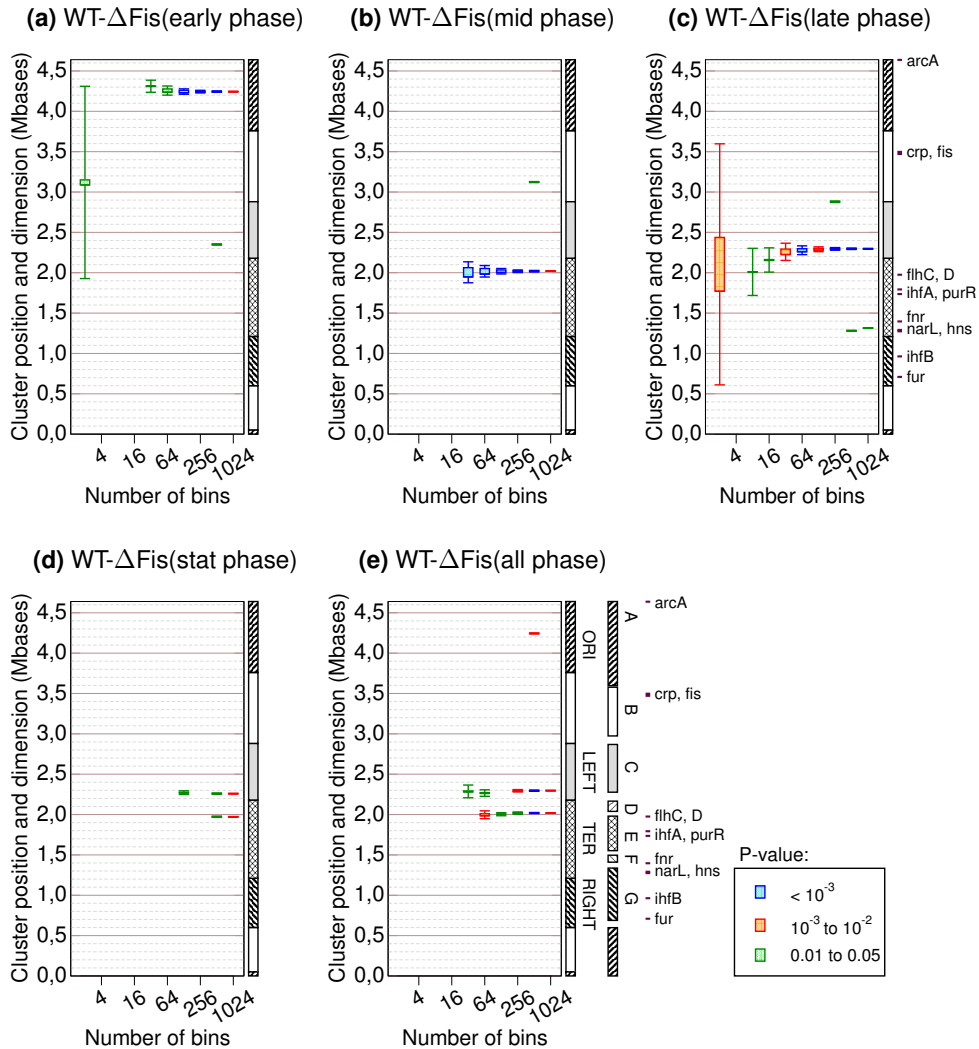
  

		Chromosomal	A		G		F		E		D		C		B	
<b>(b)</b>	<b>sector:</b>		start	end	start	end	start	end	start	end	start	end	start	end	start	end
	Position ( <i>Mb</i> )		3.59	0.59	0.68	1.33	1.40	1.49	1.54	1.97	2.03	2.16	2.27	2.86	2.97	3.57

**Supplementary Methods Table SM2** **(a)** Start and end positions in *Mb* of the macrodomains defined by Boccard and coworkers (ref. [10, 13]), and **(b)** chromosomal sectors defined by Mathelier and Carbone (ref. [37])

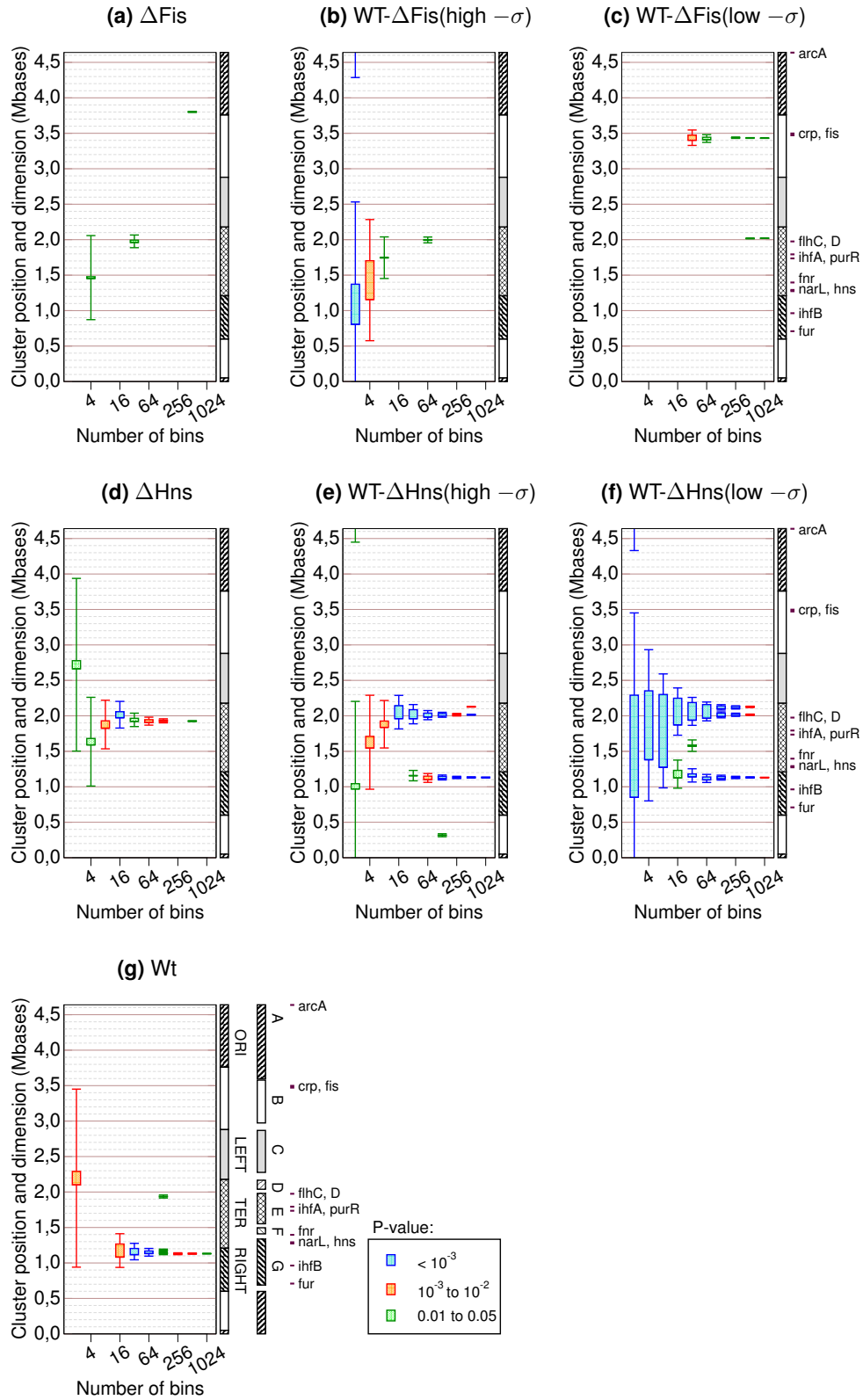
# Supplementary results for Scolari *et al*

Clusters from nucleoid perturbation / transcriptomics experiments



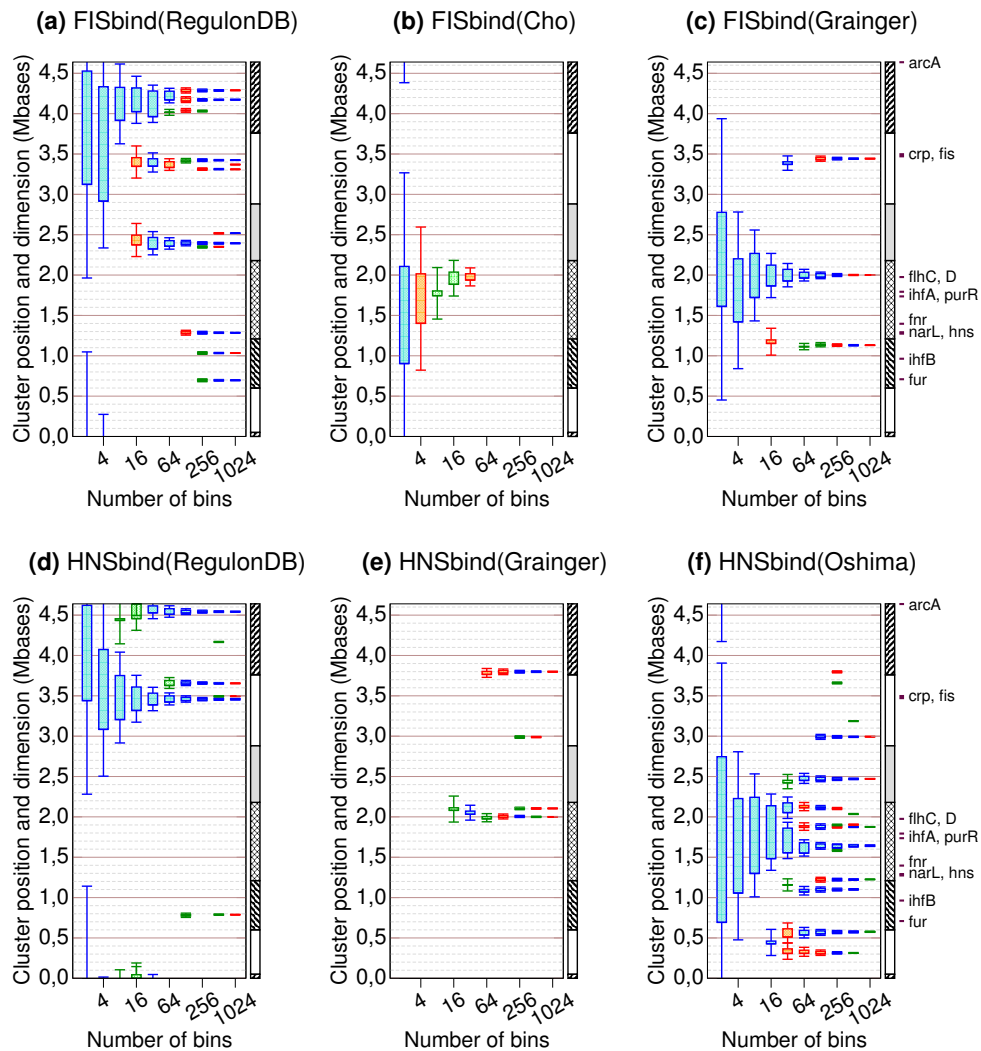
**Supplementary Figure S2** Cluster diagrams for the transcription microarray Fis deletion data from ref. [32].

Different panels refer to different growth phases (early, mid-, late-exponential and stationary, in rich media), while the last panel refers to the union of all the growth phases.



**Supplementary Figure S1** Cluster diagrams for the transcription microarray nucleoid perturbation data from ref. [30, 31].

Clusters from protein binding data:



**Supplementary Figure S3** Cluster diagrams of Fis and H-NS binding from the RegulonDB [8] database and Grainger, Cho and Oshima ChIP-chip experiments [27, 28, 57]. The binding sites of the Grainger data-set for the Fis and H-NS experiments show the same clusters as transcriptomics data on genes responding to supercoiling changes after H-NS deletion in microarray data from Marr *et al.* [30, 31]. A hypergeometric test was performed to test the overlaps of the Grainger and Cho ChIP-chip targets with the RegulonDB database (Table SM1)

Summary of clusters from transcriptomics and protein binding data:

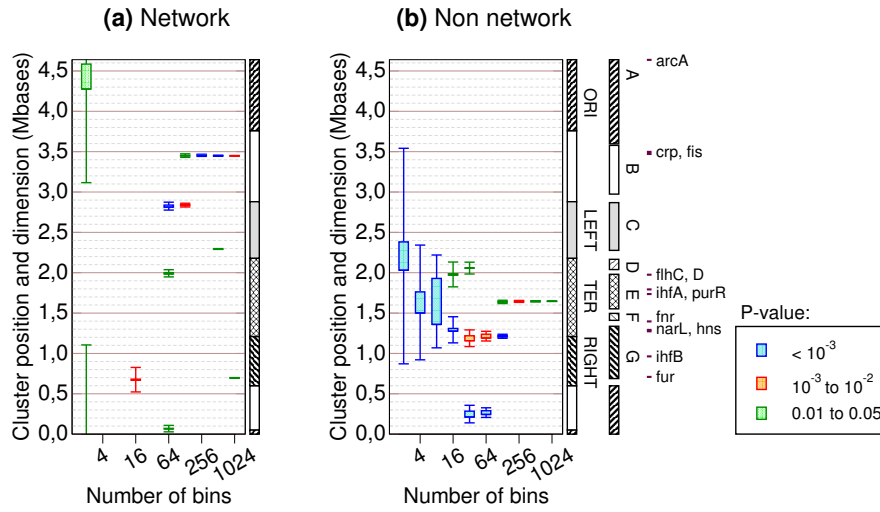
From transcriptomics:							
list	clust1	clust2	clust3	clust4	clust5	clust6	clust7
WT	0.03			< 0.001			
$\Delta$ Fis	0.05					0.04	
$\Delta$ H-NS	0.01						
WT- $\Delta$ Fis(low)	0.04	0.04			0.01		
WT- $\Delta$ Fis(high)	0.05	0.06					
WT- $\Delta$ H-NS(low)	< 0.001	< 0.001	< 0.001	< 0.001			
WT- $\Delta$ H-NS(high)	< 0.001	< 0.001	0.01	< 0.001			

From protein binding data:							
list	clust1	clust2	clust3	clust4	clust5	clust6	clust7
GraingerFis	< 0.001	< 0.001		< 0.001	< 0.001		
GraingerHns	< 0.001	< 0.001	0.01			< 0.001	0.01

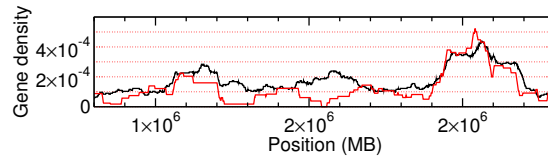
**Supplementary Table S1** Summary of the most significant clusters found at all scales and their *P*-values. The coordinates (in bp) along the *E. Coli* genome are: **Cluster 1** 1929600-2195230 **Cluster 2** 1993030-2037780 **Cluster 3** 2096110-2141990 **Cluster 4** 1094210-1163310 **Cluster 5** 3428200-3447460 **Cluster 6** 3782180-3815590 **Cluster 7** 2981340-2996630. Note: **Cluster 2** and **Cluster 3** are included in **Cluster 1**.

Clusters of genes inside and outside the known transcription regulatory network:

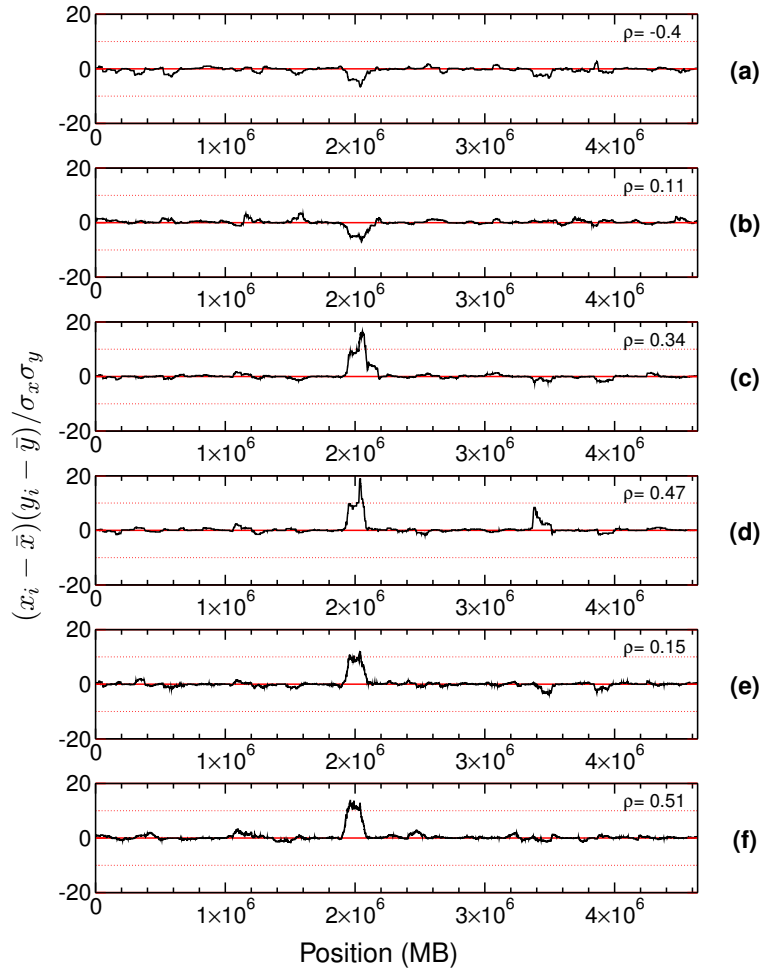


**Supplementary Figure S4** Cluster diagram of the genes in the RegulonDB network and outside RegulonDB network (see ref. [36]).

*Histograms of EPODs and comparison with clusters:*



**Supplementary Figure S5** Linear density of heEPODs along the genome (red line) compared to the density of nucleoid-perturbation sensitive genes WT- $\Delta$ H-NS(low  $-\sigma$ ) (black line, bin size  $L/32$ ). The x-axis spans the Ter macrodomain. Note the highly correlated regions at the border of the Ter (at  $1 \cdot 10^6$  and  $2 \cdot 10^6$  bases) macrodomain in accordance to the results of Figure S6.



**Supplementary Figure S6** The black lines are the local contributions to the Pearson correlation coefficient along the genome coordinate (x-axis) between the normalized linear densities of he- and tsEPODS (ref. [29]) and the densities of nucleoid-perturbation sensitive genes. The densities were calculated using a sliding window of size  $L/32$ .

**(a)** Correlation between tsEPOD and heEPOD density. **(b)** Correlation between tsEPOD density and WT- $\Delta$ H-NS(low  $-\sigma$ ). **(c)** Correlation between heEPOD and WT- $\Delta$ H-NS(low  $-\sigma$ ). **(d)** Correlation between heEPOD density and FISbinding(Grainger). **(e)** Correlation between heEPOD and FISbinding(Cho). **(f)** Correlation between FISbinding(Grainger) and FISbinding(Cho).



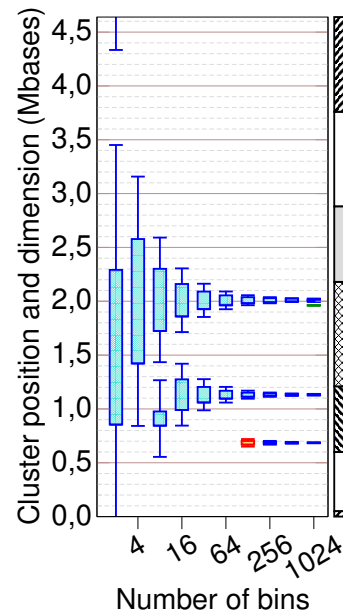
<b>Number of genes of heEPOD in common with:</b>			
List	Experimental value	Mean value	<i>P</i> -value
WT	19	16.58	0.300
$\Delta$ FIS	11	12.98	0.226
$\Delta$ HNS	15	9.06	0.034
WT- $\Delta$ FIS( $\sigma$ ↓)	22	13.29	0.004
WT- $\Delta$ HNS( $\sigma$ ↓)	31	15.64	< 0.002
WT- $\Delta$ FIS( $\sigma$ ↑)	18	8.69	< 0.002
WT- $\Delta$ HNS( $\sigma$ ↑)	30	11.52	< 0.002

**Supplementary Table S2** Summary of the number of genes within heEPODs (strictly included) in common with the genes significantly responding to Fis and H-NS deletion, and changes in supercoiling [30].

<b>Number of genes of tsEPOD in common with:</b>			
List	Experimental value	Mean value	<i>P</i> -value
WT	5	6.16	0.224
$\Delta$ FIS	7	5.43	0.298
$\Delta$ HNS	6	5.65	0.496
WT- $\Delta$ FIS( $\sigma$ ↓)	5	4.68	0.496
WT- $\Delta$ HNS( $\sigma$ ↓)	13	5.70	0.002
WT- $\Delta$ FIS( $\sigma$ ↑)	4	3.20	0.402
WT- $\Delta$ HNS( $\sigma$ ↑)	13	4.35	< 0.002

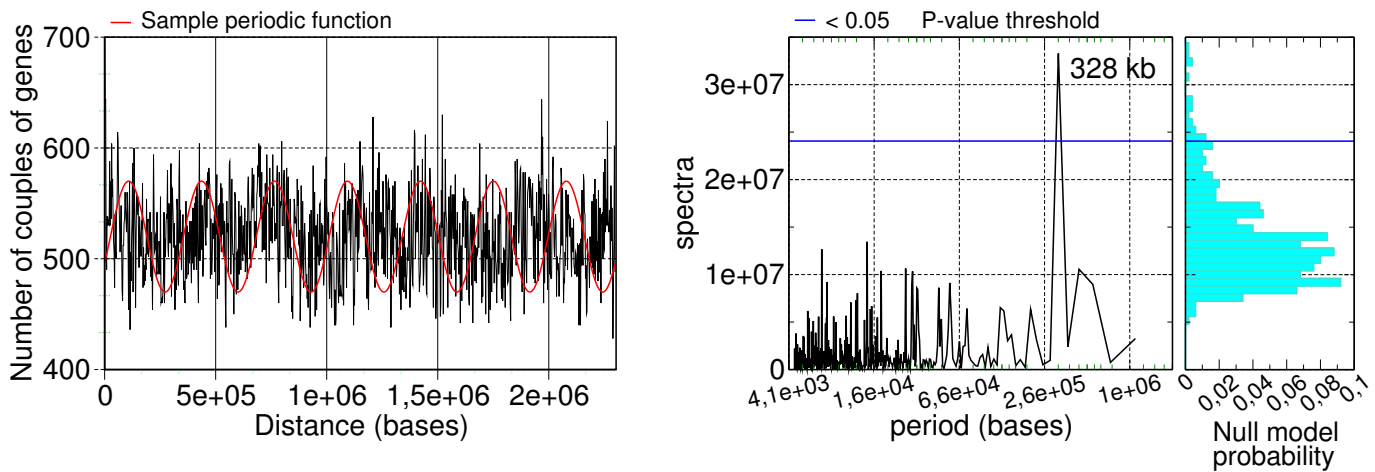
**Supplementary Table S3** Summary of the number of genes within tsEPODs (strictly included) in common with the genes significantly responding to Fis and H-NS deletion, and changes in supercoiling [30].

*Clusters of genes controlled by FlhC:*

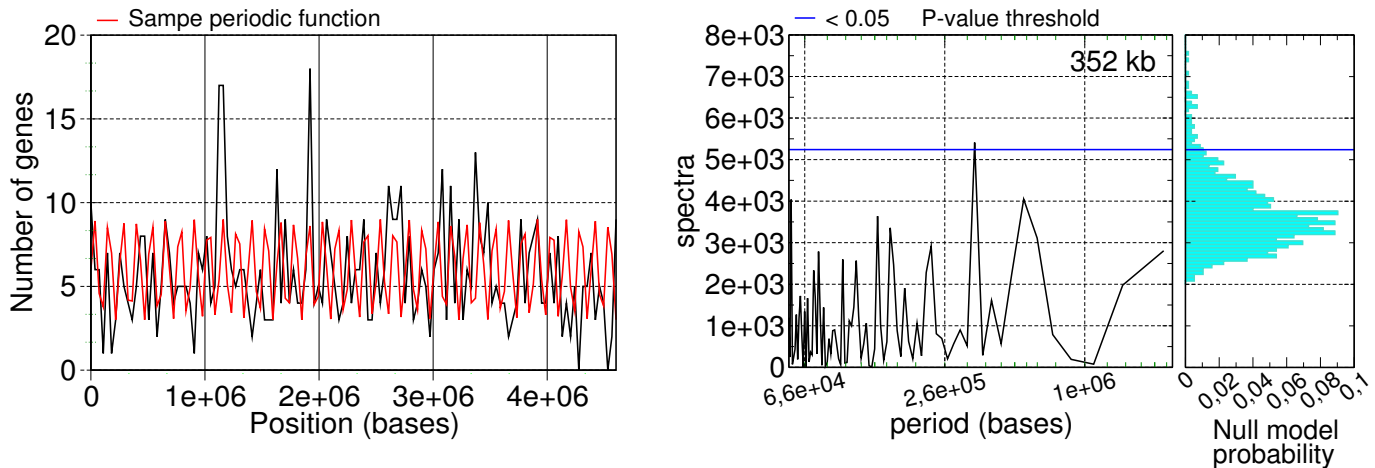


**Supplementary Figure S7** Cluster diagram of the genes controlled by the FlhC transcription factor (data from RegulonDB). FlhC is a transcriptional activator that controls the operons related to assembling of the flagella. The main regions controlled by FlhC overlaps with the clusters at the border of the Ter macrodomain identified in both transcriptomics and binding sites lists. A second cluster is present in correspondence with the border between the Right macrodomain and the Right non structured zone.

Periodicity analysis:



**Supplementary Figure S8** Procedure followed to detect periodicities in the gene lists. Left panel: distribution of the distance of genes in an experimental list (sliding window of bin-size  $L/2048$ ), compared to a periodic function. Right panel: discrete Fourier transform of the distance distribution. The peaks correspond to contributions of a periodic function of a given period, reported on the x-axis. The figure shows the spectra of the intra-strain WT list (see Methods), where the peak indicates a signal for a periodicity of 328Kb. The comparison of this signal with the distribution of the maximum of the spectra found in randomized lists gives a significance score for this periodicity. The same procedure can be applied also to the sliding-window density histogram at a given bin size.



**Supplementary Figure S9** Periodicity analysis for the case of a density histogram. The analysis (and the example dataset from the intra-strain WT list) coincides with that presented in Figure S8, except that the left panel is a sliding-window histogram (bin-size  $L/256$ ) of the genes in the list, rather than a distance distribution.

list	360 ± 36 Kb	624 ± 36Kb	101 ± 36Kb	20 ± 36Kb
WT	AB			
ΔFis			AB	
ΔH-NS				B
WT-ΔFis(low)				
WT-ΔFis(high)				
WT-ΔH-NS(low)	AB	AB	B	
WT-ΔH-NS(high)	AB	AB	B	B

**Supplementary Table S4** Table summarizing the significant periodicities found ( $P < 0.05$ ). In the table the letter A indicates a significant periodicity found in the density histogram while B indicates a periodicity found in the distance pair distribution. Genes sensitive to supercoiling variation in the intra-strain WT list show a compatible periodicity of  $360 \pm 36\text{Kb}$ , this periodicity is found also in the WT-ΔH-NS lists at all supercoiling conditions. Upon Fis deletion, supercoiling sensitive genes lose the  $360 \pm 36\text{Kb}$  periodicity, but show a new periodicity at  $101 \pm 36\text{Kb}$ , again found also in the WT-ΔH-NS lists in all supercoiling conditions. Finally, in H-NS deletion mutants, supercoiling sensitive genes lose the  $360 \pm 36\text{Kb}$  periodicity but show a periodicity at  $20 \pm 36\text{Kb}$  also found in the inter-strain WT-ΔH-NS data in high negative supercoiling conditions. The compatibility condition of  $36\text{Kb}$  was selected as twice the bin-size of the density distribution histogram.

*Clusters and the flagellar/biofilm synthesis pathway:*

**Cluster 4** 1094210-1163310

wt-fis low $\alpha$		wt-fis high $\alpha$		wt-hns low $\alpha$		wt-hns high $\alpha$	
rep	act	rep	act	rep	act	rep	act
csgA	bssS	flgA	bssS	csgD	flgA	bssS	flgA
ghrA	flgJ	flgE	flgH	csgE	flgB	csgA	flgB
grxB	flgM	ghrA	mdoC	yceI	flgC	csgB	flgC
hinT	flgN	grxB	plsX	yceJ	flgD	csgD	flgD
mdlH	plsX	hinT	yceK		flgE	csgE	flgE
rimJ		rimJ			flgF	csgG	flgF
ycdX		ycdX			flgG	mdoC	flgG
ycdY		ycdY			flgH	mdoG	flgH
yndB		ycdZ			flgI	rflC	flgI
		yclL			flgJ	yclU	flgJ
					flgM	yceJ	flgK
					flgN	yclI	flgM
					ghrA		flgN
					mdtG		holB
					yceG		yceN
					yceH		
					yceO		

**wt 41-54**      **Hns 41-54**      **Fis 41-54**

hyp		rel		hyp		rel	
csgF	flgA	csgD		csgC	flgF		
pabC	flgB	csgE		csgD	flgJ		
pyrC	flgC	csgG			mdoC		
rimJ	flgD				plsX		yclH
rflC	flgE				rimJ		
yedZ	flgF				pyrC		yceA
yceG	flgG				rimJ		yceH
yceH	flgH				yclM		yceM
yceO	flgI						yndB
	flgJ						
	flgM						

**Cluster 1** 1929600-2195230

wt-fis low $\alpha$		wt-fis high $\alpha$		wt-hns low $\alpha$		wt-hns high $\alpha$	
rep	act	rep	act	rep	act	rep	act
baeS	amyA	amn	cld	cpsB	dcm	araG	cheY
cbi	cheB	aspS	flgG	gatD	flhB	araH	dcyD
cpsB	cheZ	eda	flhJ	gatY	flhA	cpsB	flhA
dcd	flhB	fbaB	flhL	gatZ	flhC	cpsG	flhB
erhK	flhE	f1c	flhM	glf	flhD	flcI	flhE
fbaB	flhF	flu	flhN	gmd	flhE	flhA	
ftnA	flhG	flnA	flhP	gmm	flhF	flhC	
hslI	flhL	gatC	flhQ	ogrK	flhG	gatA	flhD
ruvA	flhM	gatY	flhR	rclR	flhH	gatC	flhE
wcaM	flhP	gmd	galF	rcaA	flhJ	gatD	flhF
yecM	flhQ	gnd	metG	thiD	flhK	glf	flhG
yecN	flhZ	hchA	rtbB	ugd	flhL	gmd	flhH
yegD	flhA	hisC	znuA	uvrC	flhM	gmm	flhJ
	yecR	hisD	znuC	uvrY	flhN	gnd	flhK
	yedW	hisF		wcaA	flhQ	hchA	flhL
	yeeV	hisH		wcaC	flhS	intG	flhM
	znuA	hisI		wcaD	flhZ	mdtD	flhN
		motB		wcaE	hisH	osaA	flhO
		ogrK		wcaF	motB	rcaA	flhQ
		pykA		wcaM	tar	rtbA	flhR
		ruvA		wzc	yecR	rtbB	flhS
		tar		yedV	yeeE	rtbC	flhY
		torZ		yeeN		rtbX	flhZ
		wbbK				rflC	motB
		wcal				ruvA	yecR
		wcaM				shiA	yedK
		wzc				torY	yedM
		yedF				torZ	
		yedI				ugd	
		yegD				uvrC	
		yegP				vsr	
		yegS				wbbI	
		yegV				wbbJ	

**wt 41-54**      **Hns 41-54**      **Fis 41-54**

hyp		rel		hyp		rel	
cmoA	flhJ	amn		cpsB	cmoB	flhI	
cmoB	yeeN	cmoA		cpsG	cobT	flhK	
cobS		dcm	rflC	dcm	dcm	flhR	
flhD		flhD		flhD	rcaA		
hisC		flhY	wcaB	flhD	wbbI		
hisD		gatC	wcaC	flhC	yeeN		
insF-5		gatD	wcaE	flhD	yeeR		
lpxM		gatY	wcaF	flhS	yeeT		
rtbB		gatZ	wcaJ	gatY	yegS		
yebK		hisC	wcaK	insA-5			
yecD		hisD	wcaL	lpxM			
yecN		hisF	wcaM	mtfA			
yedI		lpxM	wzc	pgsA			
yedR		motB	wzc	torZ			
yeeE		sdiA	yeeN	vsr			
yeeP		shiA	yeeU	yebK			
yeeZ		torY	yegS	yecD			
yegD		torZ	yehD	yecN			
yegW		uvrY	znuB	yedA			
yegX		vsr		znuA			
znuA		yebK					
		yecN					
		yedI					
		yedL					
		yedW					
		yegl					
		znuA					

**Color code legend**

- Flagellia
- O-antigen
- M-antigen capsid display/biofilm
- Regulator of biofilm formation
- Curti
- transcription factor

**Supplementary Table S5** Intersection between genes found in the data sets from the transcription microarray experiments of Blot et al [30] and clusters of genes identified in this analysis. The colors indicate the gene ontology class. Genes from intra-strain experiment have been divided into rel and hyp columns corresponding to gene transcripts whose expression is associated with relaxation (rel) or high negative supercoiling (hyp). The labels act and rep indicate activation and repression in inter-strain profiles.

**Flagellar gene expression cascade (by order of expression)**

Class	Gene	Cluster	Pos Regulator	Neg Regulator	Hns CC	predicted Hns site	Function
I	<i>flhCD</i>	1	Crp, Hns, s70, s54, s28	Fur, OmpR, RcsAB, IHF, LrhA			Master transcriptional regulator
II	<i>flLMNOPQR</i>	2	s70 FlhCD				Basal body hook
II	<i>flIE</i>	2	s70 FlhCD		Y	Y	
II	<i>flFGHIJK</i>	2	s70 FlhCD				
II	<i>flgA</i>	4	s70 FlhCD				Basal body hook
II	<i>flgBCDEFGHIJ</i>	4	s70 FlhCD			Y	
II	<i>flhBAE</i>	1	s70 FlhCD				
II	<i>flIA (s28)</i>	2	s28, s70 FlhCD	NsrR	Y	Y	Sigma 28
II	<i>flIZ</i>		s28, s70 FlhCD		Y	Y	Inhibitor of curli
II	<i>flIY</i>		ss				
III	<i>flgKL</i>	4	s28, s70 FlhCD				Hook
III	<i>flIDST</i>	2	s28, s70 FlhCD		Y		Hook
IIIb	<i>flIC</i>	2			Y	Y	Filament
II III	<i>flgMN</i>	4	s28, s70 FlhCD		Y	Y	Anti-sigma 28
IIIb	<i>motAB</i>	1	s28				motive force chemosensor
IIIb	<i>cheAW</i>	1	s28				
IIIb	<i>tar</i>	1	s28				
IIIb	<i>tap</i>	1	s28				
IIIb	<i>cheRBYZ</i>	1	s28				

**Genes involved in biofilm formation (in order of chromosome position)**

MD	Gene	Cluster	Regulates	Regulated by	Hns CC	predicted Hns site	Process
right	<i>yadCKLM</i>			Hns, Crp			cryptic fimbriae
	<i>sfmACDHF</i>			Hns, Crp			cryptic fimbriae
	<i>ycbQRSTUVS</i>			Hns, Crp	Y	Y	cryptic fimbriae
	<i>pgaABCD</i>	- 4		CsrA, NhaR			PGA, adhesin
	<i>csgD</i>	4	csg operon, bcs operon	OmpR, CpxR, Hns, IHF, RstA, Fis, ss, YdaM		Y	curli synthesis
	<i>bssS</i>	4					biofilm
	<i>ycgv</i>				Y	Y	cryptic adhesin
	<i>ydaM</i>						curli inhibitor
	<i>tqsa</i>						AI-2 transport, quorum sensing
	<i>uvrY/uvrC</i>	1	csrB	LexA, SdiA		Y	biofilm
ter	<i>sdiA</i>	2	uvrY, flIE				biofilm, cell division
	<i>rcaS</i>	2	wca, flIPQR et al				osmolarity, membrane perturbations
	<i>yedQ</i>	2*	c-di-GMP	ss			curli regulation
	<i>yeej</i>	1*					adhesin
	<i>flu</i>	1		OxyR, Dam			antigen 43
	<i>rfb operon</i>	3			Y	Y	O-antigen
	<i>wca operon</i>	3		RcsC/S/B/A		Y	colanic acid, M-antigen
	<i>yegE</i>	1*	c-di-GMP	ss			curli regulation
left	<i>yehABCD</i>	1		Hns, Crp	Y		cryptic fimbriae
	<i>yfaI</i>						adhesin
	<i>yfcOPQRSTUV</i>						cryptic fimbriae
	<i>yjiR</i>						
	<i>ypja</i>						adhesin
	<i>gutq</i>						
	<i>ttda</i>						
	<i>yraHIJK</i>			Hns, Crp			cryptic fimbriae
	<i>bcsABZC, EFG</i>			CsgD			cellulose
ori	<i>cysE</i>	6		Hns ?	Y	Y	LipoPolySaccaride synthesis
	<i>waaG</i>						
	<i>tnaA</i>						
	<i>rfah</i>						transcriptional antiterminator
	<i>yjhr</i>						
	<i>cpxAR</i>		motAB, cheAW, mdtA(1)			Y	envelope stress
	<i>yjbe</i>						
	<i>fumb</i>						
	<i>fimAICDFGH</i>			Hns ?		Y	fimbriae
	<i>yjiP</i>						

**Supplementary Table S6** Genes involved in flagellar expression and in biofilm formation, data from refs

[46, 63, 74–80]. Flagellar and chemotaxis genes are ordered according to the sequence of expression. Biofilm genes are ordered according to their position on the chromosome, the first column (MD) show the macrodomain in which the gene is located on the chromosome. The known factors regulating gene expression are indicated, as well as the targets of the transcription factors in the list, the abbreviation ss stands for sigma s. The presence of H-NS binding sites in the promoter region is shown in different columns whether it was determined by ChIP-chip [27] (Hns CC) or by prediction from bioinformatic sequence analysis [33] (Hns site).

**Supplementary files**

Downloadable from web site: <http://www.lgm.upmc.fr/scolarietal/>